

Driven injection of a polymer into a spherical cavity: A Langevin dynamics simulation study

Chao Wang(王超), Fan Wu(吴凡), Xiao Yang(杨肖), Ying-Cai Chen(陈英才), and Meng-Bo Luo(罗孟波)
Citation: Chin. Phys. B, 2021, 30 (**10**): 108202. DOI: 10.1088/1674-1056/abff21
Journal homepage: http://cpb.iphy.ac.cn; http://iopscience.iop.org/cpb

What follows is a list of articles you may be interested in

Morphologies of a spherical bimodal polyelectrolyte brush induced by polydispersity and solvent selectivity

Qing-Hai Hao(郝清海) and Jie Cheng(成洁)
Chin. Phys. B, 2021, 30 (**6**): 068201. DOI: 10.1088/1674-1056/abd7d2

Distribution of a polymer chain between two interconnected spherical cavities

Chao Wang(王超)†, Ying-Cai Chen(陈英才), Shuang Zhang(张爽), Hang-Kai Qi(齐航凯), and Meng-Bo Luo(罗孟波)‡
Chin. Phys. B, 2020, 29 (**10**): 108201. DOI: 10.1088/1674-1056/abaedc

Suppressing transition metal dissolution and deposition in lithium-ion batteries using oxide solid electrolyte coated polymer separator

Zhao Yan(闫昭), Hongyi Pan(潘弘毅), Junyang Wang(汪君洋), Rusong Chen(陈汝颂), Fei Luo(罗飞), Xiqian Yu(禹习谦), Hong Li(李泓)
Chin. Phys. B, 2020, 29 (**8**): 088201. DOI: 10.1088/1674-1056/ab9610

Artificial solid electrolyte interphase based on polyacrylonitrile for homogenous and dendrite-free deposition of lithium metal

Hang-Yu Xu(徐航宇), Quan Li(李泉), Hong-Yi Pan(潘弘毅), Ji-Liang Qiu(邱纪亮), Wen-Zhuo Cao(曹文卓), Xi-Qian Yu(禹习谦), Hong Li(李泓)
Chin. Phys. B, 2019, 28 (**7**): 078202. DOI: 10.1088/1674-1056/28/7/078202

Highly sensitive polymer photodetectors with a wide spectral response range

Mile Gao(高米勒), Wenbin Wang(王文斌), Lingliang Li(李凌亮), Jianli Miao(苗建利), Fujun Zhang(张福俊)
Chin. Phys. B, 2017, 26 (**1**): 018201. DOI: 10.1088/1674-1056/26/1/018201

Driven injection of a polymer into a spherical cavity: A Langevin dynamics simulation study*

Chao Wang(王超)[1,†], Fan Wu(吴凡)[1], Xiao Yang(杨肖)[1], Ying-Cai Chen(陈英才)[1], and Meng-Bo Luo(罗孟波)[2]

[1]*Department of Physics, Taizhou University, Taizhou* 318000, *China*
[2]*Department of Physics, Zhejiang University, Hangzhou* 310027, *China*

(Received 6 January 2021; revised manuscript received 27 April 2021; accepted manuscript online 8 May 2021)

The injection of a self-avoiding flexible polymer into a spherical cavity under a driving force is studied by using Langevin dynamics simulation. For given polymer length (N) and driving force (f), the polymer can be completely injected into the cavity only when the radius of the cavity is larger than a transition radius (R_{eC}). The dependence of R_{eC} on N and f can be described by a scaling relation $R_{eC} \propto N^{1/3} f^{-\delta}$. The value of δ changes from 4/15 in the small f region to 1/6 in the moderate f region due to the screening of the excluded-volume interaction between monomers. We find the complete injection time (τ) decreases monotonously with increasing the cavity radius or decreasing the polymer length. The simulation results are in good agreement with the theoretical predictions from the free energy analysis and a simple kinetic model.

Keywords: polymer, injection, simulation, free energy

PACS: 82.35.Lr, 82.20.Wt, 82.37.–j **DOI:** 10.1088/1674-1056/abff21

1. Introduction

Polymers (such as DNA and RNA) can be driven to translocate through nanopores from the *cis* space to the *trans* space. It relates to many biological processes and technological applications, such as ejection of DNA from a virus capsid into host cells,[1] transportation of proteins, and RNA through channels in biological membranes,[2–4] DNA packaging,[5–8] genome mapping,[9–12] gene therapy,[13] new method for DNA sequencing and separation,[14–23] *etc*. Accordingly, the dynamical properties of the translocation process have been studied extensively in the last two decades.

Since the size of the pore connecting the *cis* space and the *trans* space is much smaller than that of the polymer in the free space, it is very difficult for the polymer to translocate through the pore spontaneously. Therefore, polymer translocation is often driven by an external force, which can be provided by the electrical field,[20–23] the flow of fluid,[24,25] binding particles,[26–28] the attraction of the membrane on the *trans* side,[29,30] or the spatial confinement,[31–37] *etc*. In the studies of polymer translocation, the dependence of the translocation time (τ) on related parameters have attracted lots of attention.

For the case that both the *cis* space and the *trans* space are half-infinite, it was found that τ as a function of the polymer length N and the driving force f can be expressed as $\tau \propto N^{\alpha} f^{-\beta}$. For driven translocation by a transmembrane force, Kantor and Kardar predicted $\alpha = 1+\nu$, where ν is the Flory exponent.[38] However, based on the idea of tensile force propagation theory, the value of α was found to range between 2ν and $1+\nu$, depending on the strength of the driving force.[39–41] Recent simulation results showed that α changes from 1.37 for faster translocation to $1+\nu$ for slower translocation.[42–44] The value of α was also found to be dependent on the polymer-pore interaction. Specifically, $\alpha = 1.35$ for a noninteracting pore, and $\alpha = 1.22$ for strong attraction pores.[45] For the exponent β, it was predicted that $\beta \sim 1$ for small driving forces and $\beta \sim 0.8$ for large driving forces.[46–48]

The translocation time is also influenced by the confinement of the *cis* space and the *trans* space. For polymers in a confined *cis* space, the confinement of the *cis* side is conducive to the translocation process, and the polymer can escape from the *cis* side spontaneously by the so-called entropic force.[31] Park and Sung have first studied the escape of an ideal polymer from a spherical cavity through a small hole via the mean first passage time, and found that the confinement gives rise to the asymmetries of the entropic free energy landscape and then drives the polymer to the outside of the sphere.[32] It was found that there is a simple scaling relation between the translocation time (τ) and the polymer length (N), *i.e.*, $\tau \sim N^2$, for small spheres.[32] However, when the excluded volume interaction between polymer segments is taken into account, the confinement effect of the sphere on the polymer is strengthened, and several different scaling relations between the translocation time, the polymer length, and the initial volume fraction were found.[49,50] Recently, Huang and Hsiao performed an elaborate simulation study on the ejection of polymer from a spherical cavity, and showed clearly that

*Project supported by the Natural Science Foundation of Zhejiang Province, China (Grant No. LY20A040004) and the National Natural Science Foundation of China (Grant Nos. 11604232 and 11974305).

†Corresponding author. E-mail: chaowang0606@126.com

© 2021 Chinese Physical Society and IOP Publishing Ltd

the ejection process comprises mainly three stages: the prior stage, the confined stage, and the nonconfined stage.[37] In the confined stage and the nonconfined stage, the ejection velocity shows different scaling relations on the number of monomer in the sphere, respectively.[37]

On the contrary, when a polymer moves into a confined *trans* space, it will lose lots of accessible configurations, leading to a large reduction of the conformation entropy. Therefore, the confinement of the *trans* side will produce an effective resistive force on the polymer during the translocation process, and the successful translocation can be achieved only under large external driving forces.[5–8] By using the stochastic rotation dynamics algorithm, Ali *et al.* have investigated the packaging of flexible polymers into a capsid.[51] It was found that there are several pauses during the packaging process due to the motor losing grip of the monomers and the capsid's resistive force, and the packaging rate shows an approximately linear decrease with the number of packed monomers, which is in consistence with the experimental findings.[5] Moreover, the force needed to pack the chain was found to increases sharply near the full packaging.[51] Zhang and Luo have studied the driven translocation of a polymer into a circular confinement through a small pore, and found that the scaling exponent of the translocation time with the polymer length is dependent on the driving force and the monomer density of the whole polymer in the circular confinement.[52] Other studies indicated that the packaging of polymers into a cavity is a complex dynamical process, which is affected by many other factors, such as the attractive interaction between the polymer and the inner wall of the cavity,[30] the geometry of the cavity,[53–55] the flexibility of the polymer,[51,56] the temperature of the solvent,[57] the topology of the polymer,[58] *etc*.

Though the injection of polymer into a small spherical cavity has been studied by several groups, most of the works are based on an assumption that the polymer can be injected into the confinement completely under the driving force. In fact, under a constant driving force, whether the complete injection occurs or not is dependent on the polymer length and the radius of the cavity. In our recent work, we have studied the spontaneous injection of a flexible polymer into a spherical cavity from a long channel.[59] It was found that there is an obvious transition for polymer from the partial injection to the complete injection with increasing the radius of the cavity. However, the transition is not clear yet for forced cases.

In this work, the driven injection of a polymer into a spherical cavity is studied by using Langevin dynamics simulation. The transition radius of the cavity, at which the polymer changes from a partial injection state to a complete injection state, is defined based on the variation of the complete injection probability with the radius of the cavity. The dependence of the transition radius as well as the complete injection time on the polymer length and the driving force are mainly investigated. Several scaling relations are found and further confirmed by the free energy analysis and a simple kinetic model.

2. Simulation model and method

Simulations are carried out in three-dimensional (3D) space. Figure 1 shows a sketch of the model system. A half infinite space (the *cis* side) and a spherical cavity (the *trans* side) with radius R are connected by a short cylindrical channel with radius $R_{\rm p}$ and length L. The boundary of the model system (the wall, the channel and the cavity) is continuous.

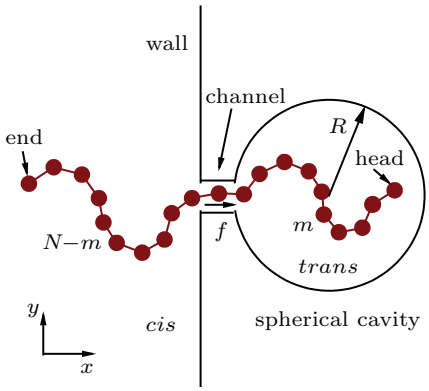


Fig. 1. A sketch of the simulation model system. The *cis* side (a half infinite space) and the *trans* side (a spherical cavity with radius R) are connected by a short cylindrical channel with radius $R_{\rm p}$ and length L. Inside the channel, each monomer of the polymer is driven by a constant force f in the direction of the x axis.

In our simulations, the polymer is modelled by a coarse-grained off-lattice bead spring model, in which the polymer with length N is composed of N identical monomers connected by bonds sequentially. The interaction between monomers is described by the repulsive Weeks–Chandler–Andersen (WCA) potential,

$$U_{\rm LJ}(r)=\begin{cases}4\varepsilon_0\left[\left(\dfrac{\sigma}{r}\right)^{12}-\left(\dfrac{\sigma}{r}\right)^{6}\right]+\varepsilon_0, & r\le r_{\rm cutoff},\\ 0, & r>r_{\rm cutoff},\end{cases} \tag{1}$$

where r is the distance between two monomers, ε_0 is the interaction strength, σ is the diameter of monomers, and $r_{\rm cutoff}=2^{1/6}\sigma$ is the cut-off distance. Moreover, there are additional interactions between bonded monomers, which are described by the finitely extensible nonlinear elastic (FENE) potential

$$U_{\rm FENE}(r)=-\frac{k}{2}R_0^2\ln\left[1-\left(\frac{r}{R_0}\right)^2\right], \tag{2}$$

where k is the spring constant, r and R_0 represent the bond length and the maximum bond length, respectively.

The interactions between monomers and the boundary of the simulation system (the wall, the channel, and the cavity) are also described by the WCA potential (Eq. (1)), where r represents the nearest distance between monomers and the boundary of the system. Besides, any monomer inside the cylindrical channel experiences a driving force $\boldsymbol{f}^{\rm dr}=f\hat{\boldsymbol{x}}$. Here, f is the

driving force strength, and $\hat{x}$ is a unit vector in the direction of the x axis. Therefore, the polymer is driven to inject into the spherical cavity.

The motion of each monomer is described by the Langevin equation

$$m\frac{\mathrm{d}\boldsymbol{v}}{\mathrm{d}t} = -\nabla(U_{\mathrm{LJ}} + U_{\mathrm{FENE}}) + \boldsymbol{f}^{\mathrm{dr}} - \eta\boldsymbol{v} + \boldsymbol{F}^{\mathrm{T}}, \tag{3}$$

where m is mass of the monomer, η is the friction coefficient, and $\boldsymbol{F}^{\mathrm{T}}$ is the random force with $\langle \boldsymbol{F}^{\mathrm{T}}(t)\rangle = 0$ and $\langle \boldsymbol{F}^{\mathrm{T}}(t)\cdot\boldsymbol{F}^{\mathrm{T}}(t')\rangle = 6\eta k_{\mathrm{B}}T\delta(t-t')$, where k_{B} is the Boltzmann constant and T is the temperature. For the numerical integration of Eq. (3), we use the velocity Verlet algorithm with a time step $\Delta t = 0.005$.

At the beginning of the simulation, the polymer is generated at the *cis* side with the head monomer in the middle of the cylindrical channel. We at first set $f = 0$ and run a long time ($> 10^6$) of Brownian motion to equilibrate the polymer under the constraint that the head monomer is fixed. Once the polymer is at the equilibrium state, we switch on the driving force and release the head monomer, and let the polymer run a long enough time ($t_{\mathrm{e}} > 10^7$) to reach the final steady-state, at which the number of packed monomers will no longer increase. We then counter the number of monomers (m_{in}) in the cavity. If $m_{\mathrm{in}} < N$, it indicates that only part of polymer is in the spherical cavity, *i.e.*, the polymer is partially injected. While if $m_{\mathrm{in}} = N$, it means that the whole polymer is in the spherical cavity, *i.e.*, the polymer is completely injected. The complete injected probability P_{in} is defined as $n_{\mathrm{w}}/n_{\mathrm{sam}}$, where n_{sam} represents the number of independent samples, and n_{w} is the number of samples satisfying $m_{\mathrm{in}} = N$. For the completely injected case, we also calculate the injection time τ, which is defined as the time interval from $m_{\mathrm{in}} = 0$ for the last time to $m_{\mathrm{in}} = N$ for the first time. During the simulation, the head monomer may go back to the *cis* side under the random thermal fluctuation, *i.e.*, the injection attempt is unsuccessful. In that failed case, we stop the simulation and begin a new simulation run. We would note that the failed samples are not counted in n_{sam}.

In this work, σ, m, and $k_{\mathrm{B}}T$ are chosen as the units of length, mass, and energy, respectively. So, the time scale and the force scale are given by $t_{\mathrm{LJ}} = (m\sigma^2/k_{\mathrm{B}}T)^{1/2}$ and $f_0 = k_{\mathrm{B}}T/\sigma$, respectively. In the simulation, we fix $\varepsilon_0 = 1$, $k = 15$, $R_0 = 2$, $\eta = 1$. Besides, to ensure the monomers of the polymer move across the channel one by one, we adopt a narrow and short cylindrical channel with $R_{\mathrm{p}} = 1.5$ and $L = 2$. In our model, the short-range repulsive interaction between polymer and the spherical cavity is WCA potential (Eq. (1)) with $r_{\mathrm{cutoff}} = 2^{1/6}\sigma$, so the distribution of monomers in the cavity with radius R is roughly confined in a spherical space with radius $R - r_{\mathrm{cutoff}}/2 \approx R - 0.56$, *i.e.*, the effective radius of the spherical cavity is $R_{\mathrm{e}} \approx R - 0.56$. This correction becomes important for the calculation of the monomer density in the cavity and the theoretical analysis in our work.

3. Results and discussion

3.1. Complete injection probability and transition radius of the cavity

Though the polymer is driven by a driving force in our work, it is not necessary that the polymer can be injected into the cavity completely. For the given polymer length and driving force, whether the complete injection could occur or not is dependent on the radius of the cavity R. Qualitatively, when R is small, there is no enough space for the cavity to accommodate the whole polymer, so it is difficult for the polymer to enter into the cavity completely. Only when R is large enough, can the whole polymer be driven into the cavity.

Figure 2 shows the dependence of the complete injection probability P_{in} on the radius of the sphere R for different polymer lengths N at $f = 0.5$. We can see two polymer states: a partial injection state with P_{in} roughly zero at small R and a complete injection state with P_{in} roughly 1 at large R. There is an obvious sharp transition from the partial injection state to the complete injection state at a special R. To give approximately the radius of the spherical cavity where the transition occurs, we here define the transition radius R_{C} at which $P_{\mathrm{in}} = 0.5$,[59] as shown in Fig. 2, and the corresponding effective transition radius is $R_{\mathrm{eC}} = R_{\mathrm{C}} - 0.56$.

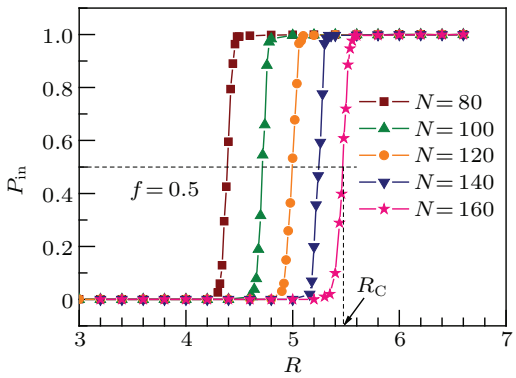


Fig. 2. The dependence of the complete injection probability P_{in} on the radius of the sphere R for different polymer lengths N, where the driving force $f = 0.5$. The radius where $P_{\mathrm{in}} = 0.5$ is defined as the transition radius R_{C}.

The effective transition radius of the cavity R_{eC} increases with N increasing, because long polymers need large cavities to accommodate all the monomers. The monotonous increase of R_{eC} with N is presented in Fig. 3 for different f. We find that R_{eC} as a function of N can be specifically expressed by a simple scaling relation $R_{\mathrm{eC}} \propto N^{0.34}$. This is different from the well known relation between the average radius of gyration (R_{g}) and the polymer length $R_{\mathrm{g}} \sim N^{\nu}$, with the Flory exponent $\nu = 0.6$ for self-avoiding polymer and 0.5 for ideal polymer. The value of ν is related to the excluded-volume interactions between different monomers and also the configurations of the

polymer. In our study, when the whole polymer is injected into the spherical cavity with radius R_{ec}, the polymer is squeezed and then the excluded-volume interaction between monomers will be partially screened, meanwhile, the polymer configurations with R_g larger than the radius of the sphere will be forbidden, which results that R_{ec} is smaller than R_g and the scaling exponent (0.34) for R_{ec} with N is smaller than ν. Quantitatively, the scaling relation between R_{ec} and N can be obtained from the free energy landscape based on the blob theory which will be shown below.

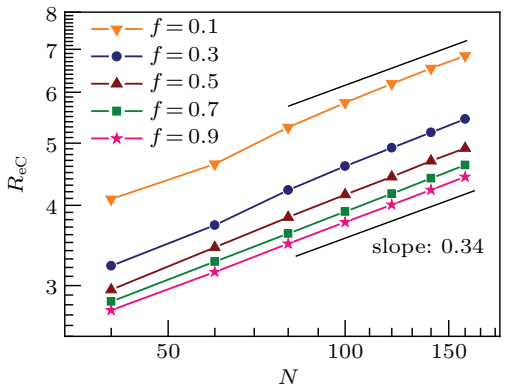


Fig. 3. The log–log plot of the effective transition radius R_{eC} *versus* the polymer length N for different driving forces f.

R_{eC} is also dependent on the driving force f. Figure 4 shows the dependence of R_{eC} on f for different N. With f increasing, R_{eC} decreases and saturates gradually at large f. In our study, due to the confinement of the cavity, the number of the configuration of polymer inside the cavity decreases, leading to an entropic force. The entropic force plays a role as a resisted force for the injection process, so the external force must be bigger than the entropic force to drive the whole polymer into the spherical cavity. Qualitatively, the entropic force is related to the radius of the spherical cavity. For large cavities, the entropic force is small, and then a relatively small driving force can driven the whole polymer into the cavity. While for small cavities, the entropic force is big, and then a large driving force is needed to complete the injection. Therefore, we find that the transition radius of the cavity decreases with the driving force increasing, *i.e.*, larger force leads to smaller transition radius for a given polymer. Specially, R_{eC} as a function of f can be expressed as $R_{eC} \propto f^{-\delta}$ in both small and moderate f regions. In the small f region ($f < 0.15$), $\delta \sim 0.27$, while in the moderate f region ($0.15 < f < 1.5$), $\delta \sim 0.17$, as shown in Fig. 4.

For any given N and f, we have also calculated the monomer density $\phi_C = N\sigma^3/8R_{eC}^3$ when the whole polymer is in the spherical cavity with the corresponding effective radius R_{eC}. ϕ_C is nearly independent of N, but it increases with f increasing and saturates gradually at large f, as shown in the inset of Fig. 4. This indicates that the polymer in the cavity is compressed gradually with f increasing. When f is large, ϕ_C is big, and then the polymer can not be compressed further, resulting that ϕ_C and R_{eC} saturate gradually at large f, as shown in Fig. 4. In small and moderate f regions, ϕ_C as a function of f can also be expressed by a scaling relation $\phi_C \propto f^{\kappa}$. Specifically, $\kappa \sim 0.8$ in the small f region ($f < 0.15$) and $\kappa \sim 0.5$ in the moderate f region ($0.15 < f < 1.5$), as shown in the inset of Fig. 4.

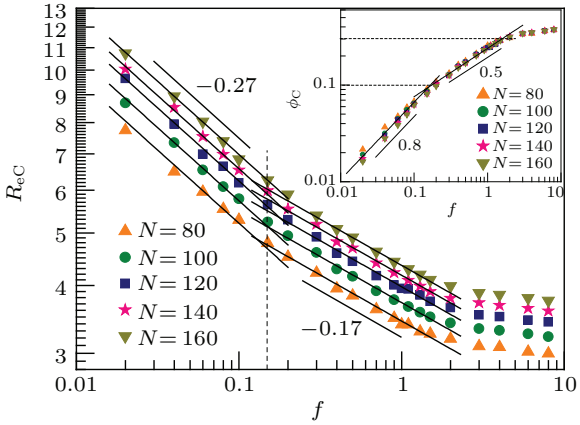


Fig. 4. The log–log plot of the effective transition radius R_{eC} *versus* the driving force f for different polymer lengths N. The inset shows the log–log plot of the monomer density ϕ_C *versus* the driving force f for different polymer lengths N.

The scaling relations of R_{eC} and ϕ_C on N and f can be understood from the free energy landscape. Assuming there are m monomers in the cavity, the free energy relative to the initial state of the injection can be expressed as[23,30]

$$F \sim C_0 m^{3\nu/(3\nu-1)} R_e^{3/(1-3\nu)} - mfL, \tag{4}$$

where C_0 is a constant and ν is the Flory exponent ($\nu = 0.6$ for self-avoiding polymer, and 0.5 for ideal polymer). In Eq. (4), the first term represents the increase in free energy due to the cost of confining m monomers in the spherical cavity with effective radius R_e,[60] and the second term is the decrease in free energy due to the work of the driving force. For any given N, R, and f, the free energy F reaches its minimum at the final steady-state, and the corresponding number of monomers (m_{in}) in the spherical cavity is determined by $(\partial F/\partial m)_{m=m_{in}} = 0$, *i.e.*,

$$m_{in} = C_1 f^{3\nu-1} R_e^3, \tag{5}$$

where $C_1 = \left(\frac{(3\nu-1)L}{3\nu C_0}\right)^{3\nu-1}$. From Eq. (5), we can define the transition radius of the sphere (R_{eC}), which satisfies $N = C_1 f^{(3\nu-1)} R_{eC}^3$, *i.e.*,

$$R_{eC} \propto N^{1/3} f^{(1-3\nu)/3}. \tag{6}$$

Obviously, the polymer can be completely injected only when $R_e \geq R_{eC}$.

For any given f, we can get from Eq. (6) that $R_{eC} \propto N^{1/3} \sim N^{0.33}$, which is in good agreement with our simulation results, as shown in Fig. 3. For any given N, we can also obtain from Eq. (6) that $R_{eC} \propto f^{(1-3\nu)/3}$ and the corresponding monomer density of the whole polymer in spherical

cavity with radius R_{eC}, $\phi_C = (N\sigma^3/8R_{eC}^3) \propto f^{3\nu-1}$. For self-avoiding polymers, the Flory exponent $\nu \sim 0.6$, so we have $R_{eC} \propto f^{-0.27}$ and $\phi_C \propto f^{0.8}$, which are in good agreement with the simulation results in small f region ($f < 0.15$), as shown in Fig. 4. With f increasing, the monomer density ϕ_C increases, and then the excluded-volume interaction between monomers is screened gradually. When the monomer density is big, the Flory exponent ν (~ 0.6) should reduce to its Gaussian value 0.5.[34] Thus, we have $R_{eC} \propto f^{-0.17}$ and $\phi_C \propto f^{0.5}$, which are in consistence with the simulation results in moderate f region ($0.15 < f < 1.5$), as shown in Fig. 4. For moderate f ($0.15 < f < 1.5$), the corresponding range of ϕ_C is about $0.1 < \phi_C < 0.3$, as shown in the inset of Fig. 4. In their work, Cacciuto and Luijten have studied the free energy of a flexible self-avoiding polymer confined in a spherical cavity, and argued that the excluded-volume interaction between monomers is screened in moderate density region $0.2 < \phi < 0.35$,[34] which is nearly the same as our result.

3.2. Complete injection time

Based on the results of R_C in Subsection 3.1, we next study the complete injection time τ for polymer injecting into spherical cavity with radius $R > R_C$. To check our simulation results, we at first calculate the complete injection time (τ_0) for the extreme case $R \to \infty$, which corresponds to the driven translocation of a polymer through a small pore connecting two half-infinite spaces. As an example, figure 5 shows the dependence of τ_0 on the polymer length N for different driving forces f and a very large $R = 10000$. We can see that τ_0 is dependent on N and f, and it as a function of N and f can be specifically expressed as $\tau_0 \propto N^{1.36} f^{-1}$, which is in good agreement with the simulation results of Luo *et al.*[44]

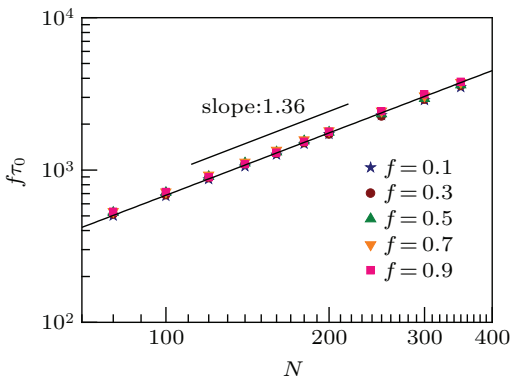


Fig. 5. The dependence of the product $f\tau_0$ on polymer length N for different driving forces f, where τ_0 represents the injection time for very large $R = 10000$.

Figure 6 shows the dependence of the injection time τ on the radius of the cavity R for different polymer lengths N. We can see that τ decreases monotonously with increasing R, due to the decrease of the confinement effect of the sphere on the polymer with R increasing. For given f and R, τ increases monotonously with increasing N, because long polymers have more monomers to be injected into the cavity. In addition, τ decreases with increasing f (results not shown), *i.e.*, the polymer moves faster and faster with the driving force increasing.

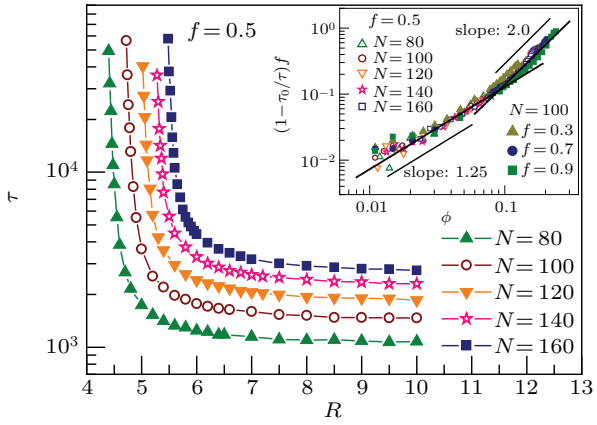


Fig. 6. The dependence of the injection time τ on the radius of the cavity R for different polymer lengths N, where the driving force $f = 0.5$. The inset shows the product $(1-\tau_0/\tau)f$ as a function of the monomer density in the cavity ϕ.

The dependence of τ on R, N, and f can be roughly understood by the following kinetic model. From Eq. (4), the increase of the free energy (ΔF) when the whole polymer is injected into the cavity can be expressed as

$$\Delta F \sim C_0 N^{3\nu/(3\nu-1)} R_e^{3/(1-3\nu)} - NfL. \tag{7}$$

We can then get the chemical potential gradient driving the injection

$$\Delta\mu = \frac{-\Delta F}{N} \sim fL - C_0 N^{1/(3\nu-1)} R_e^{3/(1-3\nu)}. \tag{8}$$

According to Kantor and Kardar,[38] the translocation time (τ) for a polymer moving across a small pore in an infinite membrane can be calculated by

$$\tau \propto \frac{R_g}{v}, \tag{9}$$

where $R_g \propto N^\nu$ represents the radius of gyration of polymer in free space, and $v \propto \Delta\mu \cdot N^{-\gamma}$ is the average velocity of the center of the mass of the polymer (several groups have argued that γ has different values, such as 1[35,38] and 0.8[36,44]).

Assuming Eq. (9) still holds in our system, the injection time can be expressed as

$$\tau \propto \frac{R_g}{v} \propto \frac{N^{\nu+\gamma}}{\Delta\mu} = \frac{N^{\nu+\gamma}}{fL(1 - C_0 N^{1/(3\nu-1)} R_e^{3/(1-3\nu)} f^{-1})}. \tag{10}$$

Obviously, the injection time τ decreases with increasing R_e (or R), which is in consistence with the simulation result as shown in Fig. 5. When $R \to \infty$, we have $R_e^{3/(1-3\nu)} \to 0$, and then $\tau \to \tau_0 \propto N^{\nu+\gamma} f^{-1} = N^{1.4} f^{-1}$ (assuming $\gamma = 0.8$[36,44]), which is in agreement with our simulation results as shown in Fig. 6. When R is finite, we can obtain from Eq. (10) that

$$\tau \propto \frac{\tau_0}{1 - C_0 N^{1/(3\nu-1)} R_e^{3/(1-3\nu)} f^{-1}}, \tag{11}$$

which can also be expressed as $(1-\tau_0/\tau)f \propto N^{1/(3\nu-1)}R_e^{3/(1-3\nu)}$ or

$$(1-\tau_0/\tau)f \propto \phi^{1/(3\nu-1)}, \tag{12}$$

where $\phi = N\sigma^3/8R_e^3$ represents the monomer density as the whole polymer is confined in the cavity.

Substituting $\nu = 0.6$ into Eq. (12), we have $(1-\tau_0/\tau)f \propto \phi^{1.25}$, which is in good agreement with the simulation result at small ϕ (< 0.1), as shown in the inset of Fig. 6. When ϕ is big, the excluded-volume interaction between monomers is screened, and the value of ν should be 0.5,[34] leading to $(1-\tau_0/\tau)f \propto \phi^2$, which is also in good agreement with the simulation result at big ϕ (> 0.1), as shown in the inset of Fig. 6.

4. Conclusion

Using Langevin dynamics simulation, we investigate the injection of a self-avoiding polymer into a spherical cavity under a driving force. With increasing the radius of the cavity, the polymer undergoes a sharp transition from the partial injection to the complete injection at the transition radius (R_{eC}). The dependence of R_{eC} on the polymer length (N) and the driving force (f) can be described by a scaling relation $R_{eC} \propto N^{1/3}f^{-\delta}$ with $\delta \sim 4/15$ for small f and $\delta \sim 1/6$ for moderate f. In addition, the monomer density (ϕ_C) of the whole polymer in the cavity with radius R_{eC} is nearly independent of N, but increases with increasing f, which can be specifically expressed as $\phi_C \propto f^{\kappa}$ with $\kappa \sim 4/5$ for small f and $\kappa \sim 1/2$ for moderate f. The scaling relations can be understood by using the free energy landscape, and the changes of values of δ and κ with f are found to be attributed to the screening of the excluded-volume interaction between monomers. The complete injection time (τ) is also calculated and found to show monotonous dependence on the polymer length, the driving force, and the radius of the cavity, which can be interpreted by a simple kinetic model.

References

[1] Laemmli U K and Favre M 1973 *J. Mol. Biol.* **80** 575
[2] Simon S M and Blobe G 1991 *Cell* **65** 371
[3] Gabashvili I S, Gregory S T, Valle M, Grassucci R, Worbs M, Wahl M C, Dahlberg A E and Frank J 2001 *Mol. Cell* **8** 181
[4] Helenius J, Ng D T W, Marolda C L, Walter P, Valvano M A and Aebi M 2002 *Nature* **415** 447
[5] Smith D E, Tans S J, Smith S B, Grimes S, Anderson D L and Bustamante C 2001 *Nature* **413** 748
[6] Fuller D N, Raymer D M, Kottadiel V I, Rao V B and Smith D E 2007 *Proc. Natl. Acad. Sci. USA* **104** 16868
[7] Fuller D N, Raymer D M, Rickgauer J P, Robertson R M, Catalano C E, Anderson D L, Grimes S and Smith D E 2007 *J. Mol. Biol.* **373** 1113
[8] Rickgauer J P, Fuller D N, Grimes S, Jardine P J, Anderson D L and Smith D E 2008 *Biophys. J.* **94** 159
[9] Levy S L and Craighead H G 2010 *Chem. Soc. Rev.* **39** 1133
[10] Lam E T, Hastie A, Lin C, Ehrlich D, Das S K, Austin M D, Deshpande P, Cao H, Nagarajan N, Xiao M and Kwok P Y 2012 *Nat. Biotechnol.* **30** 771
[11] Sriram K K, Yeh J W, Lin Y L, Chang Y R and Chou C F 2014 *Nucleic Acids Res.* **42** e85
[12] Lacroix J, Pélofy S, Blatché C, Pillaire M J, Huet S, Chapuis C, Hoffmann J S and Bancaud A 2016 *Small* **12** 5963
[13] Glasgow J and Tullman-Ercek D 2014 *Appl. Microbiol. Biotechnol.* **98** 5847
[14] Yuan Z S, Liu Y M, Dai M, Yi X and Wang C Y 2020 *Nanoscale Res. Lett.* **15** 80
[15] Wang C, Zhou Y L, Sun L Z, Chen Y C and Luo M B 2019 *J. Chem. Phys.* **150** 164904
[16] Luo K, Ala-Nissila T, Ying S and Bhattacharya A 2008 *Phys. Rev. Lett.* **100** 058101
[17] Liu X, Zhang Y, Nagel R, Reisner W and Dunbar W B 2019 *Small* **15** 1901704
[18] Luo M B and Wang C 2013 *Phys. Chem. Chem. Phys.* **15** 3212
[19] Cui R F, Chen Q H and Chen J X 2020 *Nanoscale* **12** 12275
[20] Han J and Craighead H G 2000 *Science* **288** 1026
[21] Kasianowicz J J, Brandin E, Branton D and Deamer D W 1996 *Proc. Natl. Acad. Sci. USA* **93** 13770
[22] Wang C, Chen Y C, Zhang S and Luo M B 2014 *Macromolecules* **47** 7215
[23] Magill M, Falconer C, Waller E and de Haan H W 2016 *Phys. Rev. Lett.* **117** 247802
[24] Ding M, Duan X, Lu Y and Shi T 2015 *Macromolecules* **48** 6002
[25] Li X, Pivkin I V and Liang H 2013 *Polymer* **54** 4309
[26] Ambjörnsson T, Lomholt M A and Metzler R 2005 *J. Phys.: Condens. Matter* **17** S3945
[27] Abdolvahab R H, Ejtehadi M R and Metzler R 2011 *Phys. Rev. E* **83** 011902
[28] Yu W and Luo K 2011 *J. Am. Chem. Soc.* **133** 13565
[29] Park P J and Sung W 1998 *J. Chem. Phys.* **108** 3013
[30] Sun L Z, Luo M B, Cao W P and Li H 2018 *J. Chem. Phys.* **149** 024901
[31] Turner S W P, Cabodi M and Craighead H G 2002 *Phys. Rev. Lett.* **88** 128103
[32] Park P J and Sung W 1998 *Phys. Rev. E* **57** 730
[33] Wang C, Chen Y C, Zhang S, Qi H K, Luo M B 2020 *Chin. Phys. B* **29** 108201
[34] Cacciuto A and Luijten E 2006 *Nano Lett.* **6** 901
[35] Cacciuto A and Luijten E 2006 *Phys. Rev. Lett.* **96** 238104
[36] Luo K, Metzler R, Ala-Nissila T and Ying S 2009 *Phys. Rev. E* **80** 021907
[37] Huang H C and Hsiao P Y 2019 *Phys. Rev. Lett.* **123** 267801
[38] Kantor Y and Kardar M 2004 *Phys. Rev. E* **69** 021806
[39] Sakaue T 2007 *Phys. Rev. E* **76** 021803
[40] Sakaue T 2010 *Phys. Rev. E* **81** 041808
[41] Dubbeldam J L A, Rostiashvili V G, Milchev A and Vilgis T A 2012 *Phys. Rev. E* **85** 041801
[42] Luo K, Ollila S T T, Huopaniemi I, Ala-Nissila T, Pomorski P, Karttunen M, Ying S C and Bhattacharya A 2008 *Phys. Rev. E* **78** 050901
[43] Luo K, Ala-Nissila T, Ying S C and Metzler R 2009 *Europhys. Lett.* **88** 68006
[44] Bhattacharya A, Morrison W H, Luo K, Ala-Nissila T, Ying S C, Milchev A and Binder K 2009 *Eur. Phys. J. E* **29** 423
[45] Luo M B and Cao W P 2012 *Phys. Rev. E* **86** 031914
[46] Huopaniemi I, Luo K, Ala-Nissila T and Ying S C 2006 *J. Chem. Phys.* **125** 124901
[47] Luo K, Huopaniemi I, Ala-Nissila T and Ying S C 2006 *J. Chem. Phys.* **124** 114704
[48] Luo K and Metzler R 2010 *Phys. Rev. E* **82** 021922
[49] Muthukumar M 2001 *Phys. Rev. Lett.* **86** 3188
[50] Chen Y C, Wang C and Luo M B 2007 *J. Chem. Phys.* **127** 044904
[51] Ali I, Marenduzzo D and Yeomans J M 2004 *J. Chem. Phys.* **121** 8635
[52] Zhang K and Luo K 2012 *J. Chem. Phys.* **136** 185103
[53] Ali I, Marenduzzo D and Yeomans J M 2006 *Phys. Rev. Lett.* **96** 208102
[54] Zhang K and Luo K 2013 *Soft Matter* **9** 2069
[55] Polson J M and Heckbert D R 2019 *Phys. Rev. E* **100** 012504
[56] Al-Naamani N and Ali I 2019 *Phys. Rev. E* **100** 052412
[57] Al Lawati A, Ali I and Al Barwani M 2013 *PLoS ONE* **8** e52958
[58] Nagarajan K and Chen S B 2020 *Macromol. Theor. Simul.* **29** 2000032
[59] Wang C, Wu F, Zhao B, Chen Y C and Luo M B 2020 *Macromolecules* **53** 1694
[60] Sakaue T and Raphaël E 2006 *Macromolecules* **39** 2621